

## BIOLOGICAL IMPACT OF LOW DOSE OF SUPERPARAMAGNETIC IRON OXIDE NANOPARTICLES (SPION) ON HEPG2 CELLS

---

***Carolina Barbara Nogueira de Oliveira***

Directory of Metrology Applied to Life Sciences - DIMAV, National Institute of Metrology, Quality and Technology (INMETRO), Duque de Caxias, RJ, Brazil  
Brazilian Centre for Validation of Alternative Methods - BraCVAM, Oswaldo Cruz Foundation (FIOCRUZ), Rio de Janeiro, RJ, Brazil

***Priscila Falagan- Lotsch***

Directory of Metrology Applied to Life Sciences - DIMAV, National Institute of Metrology, Quality and Technology (INMETRO), Duque de Caxias, RJ, Brazil

All content in this magazine is licensed under a Creative Commons Attribution License. Attribution-Non-Commercial-Non-Derivatives 4.0 International (CC BY-NC-ND 4.0).



**Abstract:** Superparamagnetic iron oxide nanoparticles (SPION), clinically approved metal oxide nanoparticles, hold immense potential in the biomedical field. The understanding of their impact on living systems at the cellular and molecular levels is essential for SPION efficacy and safety. To investigate the biological impact of well-characterized SPION at different doses (10 to 100µg/ml), we carried out experiments using potential target cells, hepatocytes (HepG2), to evaluate cell viability by MTT, Neutral Red and Trypan Blue assays and intracellular uptake of SPION by transmission electron microscopy. Gene expression profile and miRNA analysis were also explored. Reactive oxygen species (ROS) were evaluated using flow cytometry. Results show that SPION, even at the lowest dose, decrease cell viability assessed by MTT after 48h and induce overexpression of genes related to antioxidant pathways after 72h exposure, without changes in the miRNA expression. The significant increase in ROS production observed in doses equal to or higher than 21µg/ml of SPION is correlated with cell morphology changes induced by oxidative stress. Possibly, the increase in ROS levels leads to a modulation in the expression of oxidative stress genes in an attempt to maintain the normal redox state of cells, disregulated by SPION exposure. In a time-dependent manner, SPION accumulates inside vesicles in the cytoplasm and in the cell membrane surface. Our data confirm the oxidative stress as a mechanism of cellular toxicity triggered by SPION and also contribute to the understanding of the molecular mechanisms involved in cell response due to the SPION stimuli at low doses.

**Keywords:** metal oxide nanoparticles, Fe<sub>3</sub>O<sub>4</sub>, nanotoxicity, gene expression, oxidative stress

## INTRODUCTION

Nanotechnology and engineered nanomaterials production have stimulated massive investments worldwide, becoming a large presence in everyday life (Murphy *et al.*, 2015). By 2025, it's expected that the global value in nanotech products ranging from pharmaceuticals, industrial and food components to electronic industry elements and fine chemistry compounds will reach 350 billion dollars (Albalawi, 2021). More than 10000 tons of different engineered nanomaterials are produced or used every year worldwide, with Fe, Si, Ti, Zn, Al and Ce-oxides, Ag, quantum dots (QDs), CNT, and fullerenes being the most common nanoscale materials produced. For iron-containing nanomaterials specifically, it is estimated that more than 100 tons are produced worldwide per year (Piccinno *et al.*, 2012).

The unique properties such as superparamagnetism, high surface area and easy separation under external magnetic fields (Soenen and Cuyper, 2010, Dragar *et al.*, 2021, Meng *et al.*, 2024) give superparamagnetic iron oxide nanoparticles (SPION) immense potential for a large variety of biomedical applications. Among these applications, drug and gene delivery, tissue engineering, food analysis, photothermal therapy and cell isolation should be mentioned as the most important. Furthermore, SPION are the only clinically approved metal oxide nanoparticles for using in magnetic resonance imaging (MRI), as a contrast agent (Singh *et al.*, 2010, Wahajuddin and Arora, 2012, Xu *et al.*, 2014, Peng *et al.*, 2015, Wei *et al.*, 2021, Chen *et al.*, 2022) for example, magnetic resonance imaging, targeted delivery of drugs or genes, and in hyperthermia. Although, the potential benefits of SPION are considerable, there is a distinct need to identify any potential cellular damage associated with these nanoparticles. Besides focussing on cytotoxicity, the most

commonly used determinant of toxicity as a result of exposure to SPION, this review also mentions the importance of studying the subtle cellular alterations in the form of DNA damage and oxidative stress. We review current studies and discuss how SPION, with or without different surface coating, may cause cellular perturbations including modulation of actin cytoskeleton, alteration in gene expression profiles, disturbance in iron homeostasis and altered cellular responses such as activation of signalling pathways and impairment of cell cycle regulation. The importance of protein-SPION interaction and various safety considerations relating to SPION exposure are also addressed. Keywords: SPION; cellular stress; cytotoxicity; DNA damage (Published: 21 September 2010. Overall, it's predicted that SPION are associated with low toxicity in the human body (Al Faraj *et al.*, 2014, Malhotra *et al.* 2020, Vakili-Ghartavol *et al.* 2020, Ranjbary *et al.*, 2023). However, results remain controversial in the literature considering the difficulty to predict their potential toxic impact on the interaction with biological systems.

The great potential of SPION in biomedical applications has also highlighted their potential risks. Some studies focused on risk evaluation have shown that metal oxide NPs exposure can be dangerous and represent a real risk to humans and to the environment as well (Liu *et al.*, 2013, Llop *et al.*, 2014). According to *in vitro* and *in vivo* studies, SPION toxicity is usually based on dose-related and size-dependent effects. At high concentrations, smaller-sized NPs presented the highest risk to cause cytotoxicity (Kai *et al.*, 2011, Mahmoudi *et al.*, 2011, Zhu *et al.*, 2011). In *in vitro* assays in the presence of SPION with 5 and 20-40nm diameter showed non-toxic effects in the range of 0.1-100µg/ml in opposition to cytotoxic effects at concentrations greater than 100µg/ml in

lung adenocarcinoma, glia and breast cancer cells (Karlsson *et al.*, 2008, Ankamwar *et al.*, 2010, Singh *et al.*, 2010, Ranjbary *et al.*, 2023). However, besides the size, the cytotoxicity effects are also shape-, NP surface chemistry- and cell type-dependent (Kozissnik and Dobson, 2013). Another important point to be considered on the measurement of nanoparticles toxicity is the selection of cells that represent the organs targeted by a specific nanoparticle. Considering SPION, it is known that liver is the main organ of distribution and accumulation of this NP in the body, being hepatocytes potential targets (Ling and Hyeon, 2013, Llop *et al.*, 2014, Silva *et al.*, 2016, Vakili-Ghartavol *et al.* 2020).

Molecular mechanisms induced by SPION represent an important issue for the evaluation of their toxicity, though they remain poorly understood. An effective approach not widely explored to determine the cellular response to SPION stimuli is the evaluation of gene expression changes. Gene expression profiles are important tools to provide data that could help to understand molecular underlying basis and mechanisms among genes (Asyali *et al.*, 2006). Recent studies have reported that iron oxide nanoparticles have induced significant alterations in the gene expression levels in different cells and tissues, such as up-regulation of caspase-3 and caspase-9 genes in A549 cells (Ahamed *et al.*, 2013), overexpression of CCL-17 and IL-10 in mice's lung (Al Faraj *et al.*, 2014), rise in the mRNA levels of genes involved in stress and toxicity pathways *in vitro* (Hep3B and HT-29 cells) and *in vivo* (mice liver tissue) (Hwang *et al.*, 2012, Ranjbary *et al.*, 2023), and down-regulation of genes related to oxidative stress and metabolic processes in mice liver as well (Yang *et al.* 2015, Wei *et al.*, 2021). Besides the mRNA levels evaluation, the miRNAs analysis are also relevant since these small non-coding RNAs can regulate gene expression at the

post-transcriptional level, being essential to the regulation of several important biological processes such as cell survival, growth, differentiation and death (Tomankova *et al.*, 2010, Wang, 2010, Yokoi and Nakajima, 2011, Tan Gana *et al.*, 2012). Because of these regulatory roles, the aberrant miRNA expression has been implicated in several diseases, including cancer. The miRNAs meet many of the ideal biomarker criteria of high specificity, sensitivity, and accuracy, making them potential biomarkers for toxicity and disease (Fu *et al.*, 2011). Recently, two studies exploring the analysis of SPION toxicity by SOLiD sequencing-based miRNA expression profiling have demonstrated alterations in some miRNAs expression levels in NIH/3T3 cells and PC12 cells (Li *et al.*, 2011, Sun *et al.*, 2015). Therefore, the purpose of the present study was to evaluate the impact of SPION on liver cells using a range of doses (10 to 100µg/ml) considered non-toxic for other cells by exploring the cellular and molecular mechanisms involved in SPION exposure.

## METHODS

### SUPERPARAMAGNETIC IRON OXIDE NANOPARTICLES (SPION)

SPION (Fe<sub>3</sub>O<sub>4</sub>) of 5nm (4-6nm by TEM) were purchased from Sigma-Aldrich (Saint Louis, MO, USA) as aqueous, dark brown dispersions, stabilized by <1% of PEG (product number: 725331; lot: MKBJ6706V).

### CHARACTERIZATION OF SPION

The mean average size in high-purity water was determined by transmission electron microscopy (TEM) on a Tecnai™ Spirit Microscope (FEI Company, OR, USA) operating at 120 kV, by counting 349 random particles. The zeta potential and hydrodynamic diameter of SPION were measured using a Zetasizer Nano ZS (Malvern Instruments,

Malvern, UK). These measurements were performed immediately after the dilution of five NPs concentrations used in this study (21, 31, 46, 68 and 100µg/mL) in high-purity water and also in DMEM (Dulbecco's modified Eagle's media) with 5% FBS. The lowest concentrations (10 and 14 µg/mL) could not to be measured since polydisperse solutions were observed, resulting in a poor quality data. All solutions were measured at pH around 7.0 to 7.5.

### CELL CULTURE

HepG2 cells were provided by BCRJ (Rio de Janeiro Cell Bank, Brazil) and maintained in DMEM media, without antibiotics, supplemented with 10% fetal bovine serum (FBS). Cells were incubated at 37°C in 5% CO<sub>2</sub> air-humidified atmosphere and were passaged as needed using 0.125% trypsin-EDTA. The cell culture reagents were purchased from Life Technologies, USA. The HepG2 authenticity was determined in our laboratory via DNA fingerprinting (StemElite™ ID System - Promega, USA). *Mycoplasma* contamination screening using LookOut® Mycoplasma PCR Detection Kit (Sigma-Aldrich - Saint Louis, MO, USA) and MycoAlert™ Mycoplasma Detection (Lonza - Basel, SUI) were performed before each experiment and were *Mycoplasma*-free.

### CELL EXPOSURE

Seven different concentrations of NPs (10, 14, 21, 31, 46, 68, 100 µg/mL) were suspended in DMEM with 5% FBS just before addition to HepG2 cells. The culture media was replaced by DMEM with 5% FBS containing different concentrations of SPION 24 hours after plating the cells. The lowest and highest concentrations tested correspond to 7 and 72 µgFe/ml, respectively. Exposure was performed with 80% confluent cells. Non-treated cells were used as control.

## CYTOTOXICITY ASSAYS

Cell viability was determined by the MTT, Neutral Red (NR) uptake and Trypan blue assays, according to the manufacturer's instructions. HepG2 cells were plated into 96-well plates (10,000 cells per well) for MTT reduction and Neutral Red (NR) uptake assays and 20,000 cells per well into 24-well plates for the Trypan blue assay. After 24h, the cell culture media was replaced by the media containing the range of SPION. DMEM with 5% FBS with or without SDS (Sodium Dodecyl Sulfate, 32µg/mL) represented the positive and negative controls, respectively. After NP exposure, cells were incubated for 24, 48 and 72h. Then, cells were washed with PBS following the protocol proposed Guadagnini et al. (2013) to avoid/minimize the effects of NP on cytotoxicity assessments. All experiments were carried out in biological triplicates, with six technical replicates each.

After each incubation time, the MTT assay (3-(4,5-Dimethyl-2-thiazolyl)-2,5-diphenyl-2H-tetrazolium bromide, Sigma-Aldrich, MO, USA) was performed by adding 100 µL of MTT reagent (0.45mg/mL in PBS) to each well followed by 2h incubation. Then, 100 µL of DMSO solution was used to solubilize the formazan crystals. Also, to check some possible interference of NP with the MTT assay, three replicates of the reaction product MTT-formazan obtained from the incubation of HepG2 cells with MTT reagent were mixture with different concentrations of SPION based on Kroll et al. (2012) and Guadagnini et al. (2013) protocols. The solutions were measured in a microplate reader at 540nm (Synergy Biotek Instruments, VT, USA) and compared with no NP addition solutions (blanks).

The NR uptake assay was performed using Neutral Red-based kit (Sigma-Aldrich, USA) by adding 50µg/mL of NR dye in each well. After 2h incubation at 37°C, the dye was extracted and the uptake was quantified. For

both assays, MTT and NR, the optical density at 540nm (reference at 690nm) was measured in a microplate reader (Synergy Biotek Instruments, VT, USA).

For the Trypan blue assay, cells exposed to different NPs concentrations were trypsinized. Ten microliters (10µL) of the suspensions obtained were mixed with 10 µL of trypan blue (0.4%, Invitrogen, MA USA) and counted automatically using the Countess® Automated Cell Counter (Invitrogen, MA, USA). Cell viability was expressed based on the percentage of untreated cells (100% viable).

## INTRACELLULAR UPTAKE OF SPION

HepG2 cells ( $5 \times 10^5$  cells) were plated in 25cm<sup>2</sup> flasks. After 24h, the cell culture media was replaced by the media containing the range of SPION (10, 14, 21, 31, 46, 68 and 100µg/mL). After 72h incubation, the cells exposed to SPION and unexposed cells (control) were washed with PBS, trypsinized and fixed with 2.5% glutaraldehyde overnight at 4°C. The post-fixation was carried out with 1% osmium tetroxide and 1.25% potassium ferrocyanide for 1h. After dehydrated with series of ethanol solutions (Merck, Germany), cells were embedded in Epon resin. Ultrathin sections (100nm) were cut with EM UC7 ultramicrotome (Leica Microsystems - DE) and stained with uranyl acetate. The samples were observed on TEM Tecnai™ Spirit Microscope (FEI Company, USA), operated at 120kV. All reagents used in the microscopy analysis were purchased from Electron Microscopy Sciences (EMS, PA, USA).

## QUANTITATIVE REAL-TIME POLYMERASE CHAIN REACTION ASSAY (QRT-PCR)

Total RNA was extracted from HepG2 cells ( $1 \times 10^6$  cells) exposed to the lowest concentration of SPION ( $10\mu\text{g}/\text{mL}$ ) for 72h using miRNeasy mini kit (Qiagen, CA, USA), according to the manufacturer's instructions. Three biological replicates were carried out for exposed and non- exposed cells. The amount and purity of total RNA were evaluated with a UV spectrophotometer (NanoDrop 2000, Thermo Fisher Scientific Inc, MA, USA), by A260/280 and 260/230 ratios, considering the cut-off values equal or greater than 2.0 and 1.8, respectively. The integrity of the RNA extracted was evaluated in bleach gel stained with gel red (Biotium, CA, USA). The material was stored at  $-80^\circ\text{C}$  until ready for gene expression analysis.

For mRNA expression analysis, the cDNA was synthesized from  $1\mu\text{g}$  of total RNA by using RT<sup>2</sup> First Strand Kit (Qiagen, NL). The quantitative gene expression analysis was performed using PCR Array plates (RT<sup>2</sup> Profiler™ PCR Array Human Stress Toxicity & PathwayFinder, Qiagen, NL) containing specific primers for 84 genes related to oxidative stress, inflammatory response, osmotic stress, hypoxia, cell death (apoptosis, necrosis and autophagy), heat shock proteins and DNA damage. Melting curve analysis was performed for all samples.

For miRNA analysis, 600ng of total RNA was used for the cDNA synthesis with the TaqMan® MicroRNA Reverse Transcription Kit (Applied Biosystems, MA, USA). Custom PCR Array plates containing specific primers to detect six miRNAs, let-7a, miR17-5p, miR200c, miR146a, miR21 and, miR221 were used. These targets were selected due to their importance in inflammation, apoptosis and carcinogenesis processes. Additionally, five controls were selected as housekeeping genes;

RNU44, RNU48, U6, U47 and 18S.

The quantitative gene expression analysis was performed on ABI7500 (mRNA) or ABI7500 FAST (miRNA) equipments (Applied Biosystems, MA, USA) with cycle conditions comprised of a 10 min at  $95^\circ\text{C}$ , followed by 40 cycles of 15 s at  $95^\circ\text{C}$  and 1min at  $60^\circ\text{C}$ , according to the manufacturer.

## MEASUREMENT OF REACTIVE OXYGEN SPECIES (ROS)

For this assay, the 2',7'-dichlorodihydrofluorescein diacetate ( $\text{H}_2\text{DCFDA}$  - Invitrogen, USA) was used as the fluorescent dye. A stock solution of the dye was made by dissolving  $\text{H}_2\text{DCFDA}$  powder in absolute ethanol (Merck, Germany). The working solution ( $5\mu\text{M}$ ) was prepared using PBS (pH 7.4) as the solvent. Hydrogen peroxide ( $\text{H}_2\text{O}_2$ ) (Merck, Germany) was used as a positive control to generate stress in cells. HepG2 cells were exposed with the range of NPs (10, 14, 21, 31, 46, 68 and  $100\mu\text{g}/\text{mL}$ ). At the end of treatment, after 72h, the cells were washed thoroughly with PBS to avoid the interference with nanoparticles in the assay (Kroll *et al.*, 2012., Guadagnini *et al.*, 2013.)engineered nanoparticles are highly potential in influencing classical cytotoxicity assays. Here, four common in vitro assays for oxidative stress, cell viability, cell death and inflammatory cytokine production (DCF, MTT, LDH and IL-8 ELISA. Cells were harvested and incubated with  $5\mu\text{M}$  of  $\text{H}_2\text{DCFDA}$  for 30 min, in absense of light. Then, the cells were washed with DMEM without serum and the fluorescence was measured using flow cytometry (FACSAriaIII, BD Biosciences, USA). The measurements of solutions with nanoparticles and dye were performed as a control experiment to evaluate the interference of nanoparticles with the optical detection of DCF fluorescence in flow cytometry. All experiments were carried out

three times, independently.

## STATISTICAL ANALYSIS

All values of zeta potential, hydrodynamic diameters, cytotoxicity assays and detection of ROS were presented as mean  $\pm$  SEM. One-way ANOVA test for variance analysis followed by Dunnett's comparison tests were performed for all of these parameters with the GraphPad Prisma software version 5.03 (GraphPad Software, Inc., CA, USA).

Relative expression levels for both mRNA and miRNA were calculated to each sample after normalization against the geometric averaging of the reference genes. The  $\Delta\Delta C_t$  method was performed to compare relative fold expression differences. Statistical analysis of qRT-PCR data was performed using the Student's t-test on the web-based RT<sup>2</sup> Profiler™ PCR Array Data Analysis software (SABiosciences, [www.SABiosciences.com/pcrarraydataanalysis.php](http://www.SABiosciences.com/pcrarraydataanalysis.php)) and Expression Suite Software (version 1.0.3, Life Technologies, USA). p-values less than 0.05 were considered statistically significant.

## RESULTS

### CHARACTERIZATION OF SPION

The spherical SPION size uniformity was observed by TEM. The average diameter of the NPs was  $10.9 \pm 4.32$ nm (n= 349 measurements) (Figure 1A and 1B).

The DLS revealed that the hydrodynamic diameter of NPs was consistently  $74.5 \pm 1.8$ nm (z-average mean) and the zeta potential average was  $-25.6 \pm 1.5$ mV in water. Even in the presence of PEG to prevent particle aggregation and stabilize the solutions, NPs size and surface charge increased in the presence of DMEM with 5% FBS culture media (z-average hydrodynamic diameter of  $92.1 \pm 3.5$ nm and a zeta potential average of  $-11 \pm 0.2$ mV). Table 1 summarizes the

hydrodynamic particle size and zeta potential values obtained.

### EFFECT OF SPION ON HepG2 CELLS VIABILITY

The effect of SPION in HepG2 cells viability was first evaluated by MTT reduction assay. As a control experiment, the absorbance at 540nm of mixtures of MTT-formazan and different SPION concentrations was monitored and no interference was observed (data not shown). As shown in Figure 2, the cell viability did not decrease after 24h exposure. However, after 48 and 72h exposure, SPION at  $\geq 10\mu\text{g/ml}$  induced around 40% decline in cell viability when compared with non-exposed cells (p<0.001).

Neutral Red uptake and Trypan blue assays, used to evaluate membrane integrity, showed no significant effect upon exposition to SPION (data not shown). Furthermore, there were no significant changes in doubling time and proliferation rate of treated cells evaluated by trypan blue compared to untreated cells (data not shown).

### CELLULAR UPTAKE OF SPION

According to the TEM images obtained after 24h exposure, SPION uptake was not homogeneous among the different concentrations tested. Therefore, it was possible to observe SPION in just some cells (data not shown). Nevertheless, the incorporation of SPION by HepG2 cells could be seen in TEM images after 72h exposure in a homogeneous manner (all cells and in all concentrations tested). It is possible to observe SPION accumulation inside vesicles in the cytoplasm (Figure 3A-A1) and also presented in the cell membrane surface (Figure 3B). Moreover, myelin figures were observed in the cytoplasm of a few cells (Figure 3C). Also, some images showed membrane bleb formation suggesting stressed cells (Figure

3D-D1). These findings were not observed in untrated cells (data not shown).

## GENE EXPRESSION PROFILING

The expression of 84 genes was assessed by qRT-PCR to investigate the genetic impact of the lowest concentration of SPION (10µg/ml) on HepG2 cells exposed after 72h. The target genes are related to oxidative and osmotic stress, inflammation, hypoxia, cell death (apoptosis, necrosis and autophagy), heat shock proteins and DNA damage. A total of eight genes were overexpressed in the exposed compared to non-exposed cells, with three of them (*DNAJC3*, *GCLM* and *TXNRD1*) presenting fold-change higher than 1.5 (Table 2 and Figure 4). All of these genes are related to oxidative stress pathways.

Moreover, under the same conditions used to mRNA expression assays, miRNAs-target expression related to inflammation, cell death and carcinogenesis was evaluated and showed no significant fold-change for miR146a, miR21, miR221, miR200c, miR17-5p, and let-7a when exposed cells were compared to non-exposed (Table 3 and Figure 5).

## REACTIVE OXYGEN SPECIES DETECTION

The H<sub>2</sub>DCFDA dye allowed the measurement of the ROS generation in HepG2 cells triggered by SPION exposure. A control experiment performed confirmed no interference of NPs with the optical detection of the probe fluorescence (not shown). Intracellular ROS oxidize the dye to a green-fluorescent form detectable by flow cytometry. SPION induced a significant increase (p<0.001) in the ROS production by HepG2 cells in concentrations higher than 21µg/ml of NPs, after 72h exposure, in comparison to non-exposed cells (Figure 6). These results showed similar mean values of fluorescent units compared to 0.03% H<sub>2</sub>O<sub>2</sub>

(positive control).

## DISCUSSION

The medical, economic and technological opportunities arising from nanotechnology make it a key area for development, attracting huge investments from both public and private sectors. Iron oxide nanoparticles (SPION) amass numerous benefits concerning a variety of biomedical applications and they have been pointed out as one of the most promising types of NPs in this area. However, the potential risks of SPION in humans have not been considered with the same intensity. Due to the widespread application of nanomaterials, regulatory agencies are raising some concerns regarding nanomaterial adverse effects in human health and in the environment (Brandenberger *et al.*, 2010, Oberdörster, 2010, Rahman *et al.*, 2013, Albalawi *et al.*, 2021, Pérez-Hernández *et al.*, 2021). SPION are already used as contrast in human and animal clinical MRI analyses (Bomati-Miguel *et al.*, 2014, Xu *et al.*, 2014, Chen *et al.*, 2022, Meng *et al.*, 2024). A range of 2.5 to 56 µgFe/ml of SPION is needed for this purpose. In the present study, the dose range of NPs was selected based on the literature showing the non-toxic effect of SPION in experiments performed up to 100µg/ml of NPs in fibroblasts, glia and breast cells (Ankamwar *et al.*, 2010). We have demonstrated that even at low doses of iron (7µgFe/ml in 10µg/ml of NPs), SPION were able to induce significant decrease in cell viability assessed by MTT after 48h-exposure and also the overexpression of genes related to oxidative stress in human liver cells (HepG2) after 72h-exposure.

It has been reported that the main contributor to the toxicity observed in cells exposed to iron oxide NPs is the generation of reactive oxygen species (ROS) (Ling and Hyeon, 2013, Vakili-Ghartavol *et al.* 2020, Ranjbary *et al.*, 2023). Due to changes in gene expression in oxidative stress pathway,

flow cytometry was performed to detect the production of reactive oxygen species in cells exposed to SPION during 72h. A significant increase in ROS production was observed in doses equal to or higher than 21µg/ml of SPION. Also, we have observed the formation of myelin figures and the development of bubble-like protrusions on some cell surfaces, which can be an indicative of a morphological alteration characteristic of cell injury (Ghadially, 1988). The blebbing is a phenomenon that occurs during hypoxia, ATP depletion or oxidative stress, and it also has been associated with apoptosis or necrosis (Gores *et al.*, 1990, Lane *et al.*, 2005, Tsai *et al.*, 2010).

ROS can be generated intrinsically or extrinsically in response to various stimuli in the cells and can act as a protective or injurious molecule to cell signaling and homeostasis processes (Huang *et al.*, 2010, Manke *et al.*, 2013, Kawagishi and Finkel, 2014). Alterations in ROS levels associated with an imbalance in antioxidant defense capacity of cells may lead to an oxidative stress that could trigger a variety of events including DNA damage and cell death (Manke *et al.*, 2013, Periasamy *et al.*, 2014, Vakili-Ghartavol *et al.* 2020, Wei *et al.*, 2021, Ranjbary *et al.*, 2023).

Mitochondria, redox-active organelles, are identified as prominent site of ROS formation induced by nanoparticles exposure. After internalization, SPION seems to be degraded into iron ions in lysosomes (Singh *et al.*, 2010) and the excess of free Fe ions may potentially overpass the nuclear or mitochondrial membrane, resulting in oxidative stress and cellular damage (Huang *et al.*, 2013). Our results suggest that SPION affect the HepG2 cellular viability by disrupting mitochondria activity measured by MTT assay after 48h of exposure. Similar results in cell viability, measured by MTT method and in accordance with other assays, were described in other

studies evaluating higher concentrations or larger diameter iron oxide nanoparticles in *in vitro* models using different cell types. J774 cells exposed up to 200µg/mL of SPION (30nm) show a significant reduction of around 40% in cell viability after six hours exposure (Naqvi *et al.*, 2010). A549 cells showed a decrease in cell viability when exposed to SPION (22nm) as well. In this cell type, concentrations higher than 50µg/mL have shown a percentage decrease of 35% in cellular viability (Dwivedi *et al.*, 2014). Moreover, a reduction of at least 20% in viability of MCF-7 cell line was observed using concentrations higher than 30 µg/mL of SPION with 20-50nm diameter after 24 and 48h exposure (Alarifi *et al.*, 2014)we explored the underlying mechanism through which iron oxide nanoparticles induce toxicity in human breast cancer cells (MCF-7).

To ensure the accurate assessment of NPs toxicity, it is essential a careful validation of the test systems used. The interference of some NPs, including SPION, with several cytotoxicity assays based on colorimetric detection such as MTT as well as the NPs interaction with fluorescent dyes is well reported in the literature (Kroll *et al.*, 2012, Guadagnini *et al.*, 2013, Ong *et al.*, 2014). Thus, it is worth mentioning that to prevent/minimize the interference of SPION with the assays performed, the adaptation in the MTT and ROS detection (by H2DCFDA dye) protocols proposed by Guadagnini *et al.* (2013) suggesting multiple washing steps was performed. Control experiments were carried out to confirm the no interference of SPION with MTT assay and DCF dye in the present study (data not shown).

The gene expression profile analysis showed overexpression of genes involved in oxidative stress at the lowest dose tested, 7µgFe/ml (10µg/ml of NPs). Two genes that have presented significant altered levels, *GCLM* and *TXNRD1*, were associated to

Glutathione (GSH) and Thioredoxin (TXN) systems, which coordinate the removal of reactive oxygen (ROS) and nitrogen (RNS) species protecting the cells against oxidative stress in different organisms (Weldy *et al.*, 2012). Possibly, the modulation in the expression of such genes is induced to answer an increase in levels of oxidative stress in an attempt to maintain the normal redox state of cells, trying to protect themselves against the stress caused by SPION exposure.

The GSH and TXN systems have many overlapping functions and in most cases work in parallel, or act as a backup system for each other (Cai *et al.*, 2012, Lu and Holmgren, 2014). GSH is the most abundant cellular non-protein thiol in mammalian tissues, especially in liver, and plays a important role in antioxidative and cellular redox processes through efficient scavenging of various reactive oxygen species such as hydrogen peroxide and phospholipid hydroperoxides (Weldy *et al.*, 2012). Moreover, GSH is also known to modulate inflammatory responses and to protect against inflammatory pathologies (Sikalidis *et al.*, 2014)we investigated whether induction of GSH synthesis in response to sulfur amino acid deficiency is mediated by the decrease in cysteine levels or whether it requires a decrease in GSH levels per se. Both the glutamate-cysteine ligase catalytic (GCLC. Some studies have shown that GSH plays a critical role in determining the degree of antioxidative cellular response in several tissues after exposure to nano-sized aerosols from the ambient environment (Zhang *et al.*, 2012), CdSe/ZnS quantum dots (McConnachie *et al.*, 2013) concerns exist regarding their potential toxicity, specifically their capacity to induce oxidative stress and inflammation. In this study we synthesized CdSe/ZnS core/shell QDs with a tri-n-octylphosphine oxide, poly(maleic anhydride-alt-1-tetradecene, carbon black (Cao *et al.*,

2014) and silica NPs (Mendoza *et al.*, 2014). The *GCLM* gene encodes a glutamate-cysteine ligase subunit in mammals. The *GCLM* subunits were associated with changes in kinetic properties to enhance glutamate-cysteine ligase (GCL) activity which is the first rate-limiting enzyme in glutathione (GSH) biosynthesis. Alterations in *GCLM* expression would be expected to affect cellular GCL activity in cells and consequently affect the glutathione (GSH) biosynthesis (Sikalidis *et al.*, 2014)we investigated whether induction of GSH synthesis in response to sulfur amino acid deficiency is mediated by the decrease in cysteine levels or whether it requires a decrease in GSH levels per se. Both the glutamate-cysteine ligase catalytic (GCLC. The *TXNRD1* gene encodes a member of the family of pyridine nucleotide oxidoreductases, thioredoxin reductase 1. Thioredoxin (TrxR) in association with NADPH is responsible to form the thioredoxin system (TXN) (Holmgren and Lu, 2010). Thioredoxin reductase is a key enzyme in intracellular redox environment regulation (Raninga *et al.*, 2014). With a fast reaction rate, this enzyme acts by removing the reactive oxygen and nitrogen species for protection against oxidative stress (Cai *et al.*, 2012, Lu and Holmgren, 2014). Therefore, the increase in the transcript levels of *GCLM* and *TRXR1* observed in our study may suggest that even with no statistical significance in ROS production at 10µg/ml of SPION, these genes may be overexpressed to regulate the redox balance and to promote the detoxification in HepG2 cells caused by SPION presence.

Another alteration caused by stress conditions is the increased production of heat shock proteins. A 1.5-fold increase in *DNAJC3* gene expression levels can indicate that the endoplasmic reticulum of HepG2 cells were under stress conditions and may result in cell injury or misfolded proteins if exposed to SPION for a major period of time. The

endoplasmic reticulum (ER) is responsible for newly synthesized polypeptide chains folding and posttranslational modification. Therefore, perturbation in the protein maturation process can result in accumulation of unfolded protein into cells, disturbing cell metabolism. The DNAJC3 is a co-chaperone, originally identified in the cytosol and can be translocate to the ER upon stress (Rutkowski *et al.*, 2007). In addition, recent studies have shown that this protein can act as a molecular chaperone by interacting with unfolded proteins and preventing protein aggregation (Boriushkin *et al.*, 2014). During ER stress, DNAJC3 upregulation plays a central role in misfolded protein refolding, restoring the ER homeostasis (Gupta *et al.*, 2010) the process of mitochondrial outer membrane permeabilization (MOMP). Thus, a significant increase in DNAJC3 levels may represent an initial mechanism to restoring homeostasis in the NP-exposed cells even without detectable changes in cell metabolism.

The levels of miRNA involved in cell death, inflammation and carcinogenesis did not shown significant changes when cells exposed to 10µg/ml of SPION were compared to untreated cells. However, Li et al (2011) have reported a dysregulation of miRNAs related to cell death, metabolism and cell cycle, such as, let-7a; mir17; mir125; mir155, in 3T3 cells exposed to SPION. A recent study carried out by Sun et al (2015) also has demonstrated that miRNAs expression pattern in genes related to cell death or apoptosis pathways are widely changed in PC12 cells treated with SPION. These results suggest that SPION could trigger epigenetic effects by deregulating miRNA levels (Li *et al.*, 2011, Balansky *et al.*, 2013).

It's important to note that before assessing the potential cytotoxicity and gene expression profile of cells exposed to SPION, physicochemical characterization of size and surface charge of NPs was performed through

TEM, DLS and zeta potential techniques. The hydrodynamic particle size and zeta potential are important parameters which enable the identification of agglomerarion, aggregation, dissolution and stability of NPs in different environments. These characterizations are essential in biomedical research for validation and better interpretation of results (Wells *et al.*, 2011, Sharma *et al.*, 2014). Our DLS results have been supported by other studies which show a tendency of SPION to form aggregates in cell culture media due to the presence of proteins, amino acids and ions (Etheridge *et al.*, 2014, Sharma *et al.*, 2014). The small increase in hydrodynamic size when SPION were diluted in DMEM 5% FBS can probably be attributed to aggregation or formation of protein corona around the particles (Laurent *et al.*, 2014).

The uptake of metal oxide NPs is important for cytotoxicity evaluation and depends on the physicochemical characteristics of the NPs such as size, composition, polydispersity, surface chemistry and the interaction with other molecules (Singh *et al.*, 2010, Wei *et al.*, 2021). Once the nanoparticles were internalized, cellular processes can be altered (Sun *et al.*, 2015). Our uptake findings have demonstrated the presence of NPs inside vesicles in the cells after 72h, in all concentrations tested. Despite the aggregation state of NPs it seems that did not interfere with the uptake of SPION by the HepG2 cells since a large amount of NP have been internalized.

## CONCLUSIONS

The present study investigated the effects of SPION exposure on potential target cells (HepG2) using cytotoxicity endpoints and gene expression approaches. In light of this, our results suggest that at the lowest dose tested, 10µg/ml, SPION caused cytotoxicity and presented an impact on the expression of genes involved in oxidative stress pathways

such as *GCLM*, *TXNRD1* and *DNAJC3*. These alterations at the genomic level can be related to an attempt to maintain the normal redox equilibrium of cells, protecting themselves against the stress caused by SPION exposure.

The increase in intracellular ROS generation and morphological changes characteristic of cell injury confirmed the oxidative stress as a mechanism of cellular toxicity triggered by SPION. Furthermore, our findings contribute to the understanding of the molecular mechanisms involved in cell response due to the SPION stimuli. Indeed, further studies focused on *in vivo* models and long-term exposure using different cell types should be conducted to a complete understand of the toxicity cause by SPION.

## ACKNOWLEDGMENTS

This work was supported by the CNPq/PROMETRO (grant number 563165/2010-3), Conselho Nacional de Desenvolvimento

Científico e Tecnológico (CNPq), Fundação de Amparo à Pesquisa do Estado do Rio de Janeiro (FAPERJ), Financiadora de Estudos e Projetos (FINEP) and Instituto Nacional de Metrologia, Qualidade e Tecnologia (INMETRO). C.B.N.O was supported by Coordenação de Aperfeiçoamento de Pessoal de Nível Superior (CAPES) PhD fellowship. P.F.-L. acknowledges the CNPq/PROMETRO (382783/2013-1). The authors thank Dr Leandra Batista (Federal University of Rio de Janeiro) for the support in the flow cytometry experiments; Marcelle Pegurier (Ph.D student, Fluminense Federal University) and Elissa Grzincic (PhD student, University of Illinois Urbana-Champaign) for the English language review.

## CONFLICT OF INTEREST

The authors declare that they have no conflicts of interest.

## REFERENCES

- Ahamed M, Alhadlaq HA, Alam J, Majeed Khan M, Ali D, Alarafi S. 2013. Iron Oxide Nanoparticle-induced Oxidative Stress and Genotoxicity in Human Skin Epithelial and Lung Epithelial Cell Lines. *Curr Pharm Des* 19:(37) 6681-6690.
- Alarifi S, Ali D, Alkahtani S, Alhader MS. 2014. Iron oxide nanoparticles induce oxidative stress, DNA damage, and caspase activation in the human breast cancer cell line. *Biol Trace Elem Res* 159:(1-3) 416-424.
- Albalawi F, Hussein MZ, Fakurazi S, Masarudin MJ. Engineered Nanomaterials: The Challenges and Opportunities for Nanomedicines. *Int J Nanomedicine*. 2021 Jan 8;16:161-184.
- Ankamwar B, Lai TC, Huang JH, Liu RS, Hsiao M, Chen CH, Hwu YK. 2010. Biocompatibility of Fe(3)O(4) nanoparticles evaluated by in vitro cytotoxicity assays using normal, glia and breast cancer cells. *Nanotechnology* 21:(7) 75102.
- Asyali MH, Colak D, Demirkaya O, Inan MS. 2006. Gene Expression Profile Classification: A Review. *Curr Bioinform* 1:(1) 55-73.
- Balansky R, Longobardi M, Ganchev G, Iltcheva M, Nedyalkov N, Atanasov P, Toshkova R, De Flora S, Izzotti A. 2013. Transplacental clastogenic and epigenetic effects of gold nanoparticles in mice. *Mutat Res - Fundam Mol Mech Mutagen* 751-752:(1) 42-48.
- Bomati-Miguel O, Miguel-Sancho N, Abasolo I, Candiota AP, Roca AG, Acosta M, Schwartz S, Arus C, Marquina C, Martinez G, Santamaria J. 2014. Ex vivo assessment of polyol coated-iron oxide nanoparticles for MRI diagnosis applications: Toxicological and MRI contrast enhancement effects. *J Nanoparticle Res* 16:(3).
- Boriushkin E, Wang JJ, Zhang SX. 2014. Role of p58IPK in Endoplasmic Reticulum Stress- associated Apoptosis and Inflammation. *J Ophthalmic Vis Res* 9:(1) 134-143.
- Brandenberger C, Rothen-Rutishauser B, Mühlfeld C, Schmid O, Ferron G a., Maier KL, Gehr P, Lenz a. G. 2010. Effects and uptake of gold nanoparticles deposited at the air-liquid interface of a human epithelial airway model. *Toxicol Appl Pharmacol* 242:(1) 56-65.

- Cai W, Zhang L, Song Y, Wang B, Zhang B, Cui X, Hu G, Liu Y, Wu J, Fang J. 2012. Small molecule inhibitors of mammalian thioredoxin reductase. *Free Radic Biol Med* 52:(2) 257-265.
- Cao Y, Roursgaard M, Danielsen PH, Møller P, Loft S. 2014. Carbon Black Nanoparticles Promote Endothelial Activation and Lipid Accumulation in Macrophages Independently of Intracellular ROS Production. *PLoS One* 9:(9) e106711.
- Chen C, Ge J, Gao Y, Chen L, Cui J, Zeng J, Gao M. Ultrasmall superparamagnetic iron oxide nanoparticles: A next generation contrast agent for magnetic resonance imaging. *Wiley Interdiscip Rev Nanomed Nanobiotechnol.* 2022 Jan;14(1):e1740.
- Dragar Ć, Kralj S, Kocbek P. Bioevaluation methods for iron-oxide-based magnetic nanoparticles. *Int J Pharm.* 2021 Mar 15;597:120348.
- Dwivedi S, Siddiqui M a., Farshori NN, Ahamed M, Musarrat J, Al-Khedhairi A a. 2014. Synthesis, characterization and toxicological evaluation of iron oxide nanoparticles in human lung alveolar epithelial cells. *Colloids Surfaces B Biointerfaces* 122:209-215.
- Etheridge M, Hurley K, Zhang J, Jeon S, Ring H, Hogan C, Haynes C, Garwood M, Bischof J. 2014. Accounting for biological aggregation in heating and imaging of magnetic nanoparticles. *Technology* 2:(3).
- Al Faraj A, Shaik AP, Shaik AS. 2014. Effect of surface coating on the biocompatibility and in vivo MRI detection of iron oxide nanoparticles after intrapulmonary administration. *Nanotoxicology* 1-10.
- Fu SW, Chen L, Man Y-G. 2011. miRNA Biomarkers in Breast Cancer Detection and Management. *J Cancer* 2:116-122.
- Ghadially FN. 1988. Myelinoid membranes, myelin figures, and myelinosomes. In: *Ultrastructural Pathology of the Cell and Matrix* Volume 2. 646- 659.
- Gores GJ, Herman B, Lemasters JJ. 1990. Plasma membrane bleb formation and rupture: a common feature of hepatocellular injury. *Hepatology* 11:(4) 690-698.
- Guadagnini R, Halamoda Kenzaoui B, Cartwright L, Pojana G, Magdolenova Z, Bilanicova D, Saunders M, Juillerat L, Marcomini A, Huk A, Dusinska M, Fjellsbø LM, Marano F, Boland S. 2013. Toxicity screenings of nanomaterials: challenges due to interference with assay processes and components of classic in vitro tests. *Nanotoxicology.* 9(S1):13-24.
- Gupta S, Cuffe L, Szegezdi E, Logue SE, Neary C, Healy S, Samali A. 2010. Mechanisms of ER stress-mediated mitochondrial membrane permeabilization. *Int J Cell Biol* 2010 Article ID 170215.
- Holmgren A, Lu J. 2010. Thioredoxin and thioredoxin reductase: Current research with special reference to human disease. *Biochem Biophys Res Commun* 396:(1) 120-124.
- Huang G, Chen H, Dong Y, Luo X, Yu H, Moore Z, Bey E a., Boothman D a., Gao J. 2013. Superparamagnetic iron oxide nanoparticles: Amplifying ros stress to improve anticancer drug efficacy. *Theranostics* 3:(2) 116-126.
- Huang Y-W, Wu C, Aronstam RS. 2010. Toxicity of Transition Metal Oxide Nanoparticles: Recent Insights from in vitro Studies. *Materials (Basel)* 3:(10) 4842-4859.
- Hwang DW, Lee DS, Kim S. 2012. Gene Expression Profiles for Genotoxic Effects of Silica-Free and Silica-Coated Cobalt Ferrite Nanoparticles. *J Nucl Med* 53:(1) 106-112.
- Kai W, Xiaojun X, Ximing P, Zhenqing H, Qiqing Z. 2011. Cytotoxic effects and the mechanism of three types of magnetic nanoparticles on human hepatoma BEL-7402 cells. *Nanoscale Res Lett* 6:(1) 480.
- Karlsson HL, Cronholm P, Gustafsson J, Moller L. 2008. Copper oxide nanoparticles are highly toxic: A comparison between metal oxide nanoparticles and carbon nanotubes. *Chem. Res Toxicol* 21:(9) 1726-1732.
- Kawagishi H, Finkel T. 2014. ROS and disease: finding the right balance. *Nat Med* 20:(7) 711-3.
- Kozissnik B, Dobson J. 2013. Biomedical applications of mesoscale magnetic particles. *MRS Bull* 38:(11) 927-932.
- Kroll A, Pillukat MH, Hahn D, Schnekenburger J. 2012. Interference of engineered nanoparticles with in vitro toxicity assays. *Arch Toxicol* 86:(7) 1123-1136.
- Lane JD, Allan VJ, Woodman PG. 2005. Active relocation of chromatin and endoplasmic reticulum into blebs in late apoptotic cells. *J Cell Sci* 118:(Pt 17), 4059-4071.

- Laurent S, Saei AA, Behzadi S, Panahifar A, Mahmoudi M. 2014. Superparamagnetic iron oxide nanoparticles for delivery of therapeutic agents: opportunities and challenges. *Expert Opin Drug Deliv* 11:1-22.
- Li S, Wang H, Qi Y, Tu J, Bai Y, Tian T, Huang N, Wang Y, Xiong F, Lu Z, Xiao Z. 2011. Assessment of nanomaterial cytotoxicity with SOLiD sequencing-based microRNA expression profiling. *Biomaterials* 32:(34) 9021-9030.
- Ling D, Hyeon T. 2013. Chemical design of biocompatible iron oxide nanoparticles for medical applications. *Small* 9:(9-10) 1450-1466.
- Liu G, Gao J, Ai H, Chen X. 2013. Applications and potential toxicity of magnetic iron oxide nanoparticles. *Small* 9:(9-10) 1533-1545.
- Llop J, Estrela-Lopis I, Ziolo RF, González A, Fleddermann J, Dorn M, Vallejo VG, Simon-Vazquez R, Donath E, Mao Z, Gao C, Moya SE. 2014. Uptake, biological fate, and toxicity of metal oxide nanoparticles. *Part Part Syst Charact* 31:(1) 24-35.
- Lu J, Holmgren A. 2014. The thioredoxin antioxidant system. *Free Radic Biol Med* 66:75-87.
- Mahmoudi M, Laurent S, Shokrgozar M a., Hosseinkhani M. 2011. Toxicity evaluations of superparamagnetic iron oxide nanoparticles: Cell 'vision' versus physicochemical properties of nanoparticles. *ACS Nano* 5:(9) 7263-7276.
- Malhotra N, Lee JS, Liman RAD, Ruallo JMS, Villaflores OB, Ger TR, Hsiao CD. Potential Toxicity of Iron Oxide Magnetic Nanoparticles: A Review. *Molecules*. 2020 Jul 10;25(14):3159.
- Manke A, Wang L, Rojanasakul Y. 2013. Mechanisms of nanoparticle-induced oxidative stress and toxicity. *Biomed Res Int Article ID* 942916.
- McConnachie L a., Botta D, White CC, Weldy CS, Wilkerson HW, Yu J, Dills R, Yu X, Griffith WC, Faustman EM, Farin FM, Gill SE, Parks WC, Hu X, Gao X, Eaton DL, Kavanagh TJ. 2013. The Glutathione Synthesis Gene *Gclm* Modulates Amphiphilic Polymer-Coated CdSe/ZnS Quantum Dot-Induced Lung Inflammation in Mice. *PLoS One* 8:(5) 1-11.
- Meng YQ, Shi YN, Zhu YP, Liu YQ, Gu LW, Liu DD, Ma A, Xia F, Guo QY, Xu CC, Zhang JZ, Qiu C, Wang JG. Recent trends in preparation and biomedical applications of iron oxide nanoparticles. *J Nanobiotechnology*. 2024 Jan 8;22(1):24.
- Mendoza A, Torres-Hernandez J a, Ault JG, Pedersen-Lane JH, Gao D, Lawrence D a. 2014. Silica nanoparticles induce oxidative stress and inflammation of human peripheral blood mononuclear cells. *Cell Stress Chaperones* 777-790.
- Murphy CJ, Vartanian AM, Geiger FM, Hamers RJ, Pedersen J, Cui Q, Haynes CL, Carlson EE, Hernandez R, Klaper RD, Orr G, Rosenzweig Z. 2015. Biological Responses to Engineered Nanomaterials: Needs for the Next Decade. *ACS Cent Sci* 1:(3) 117-123.
- Naqvi S, Samim M, Abdin MZ, Ahmed FJ, Maitra a. N, Prashant CK, Dinda AK. 2010. Concentration-dependent toxicity of iron oxide nanoparticles mediated by increased oxidative stress. *Int. J. Nanomedicine* 5:(1) 983-989.
- Oberdörster G. 2010. Safety assessment for nanotechnology and nanomedicine: Concepts of nanotoxicology. *J Intern Med* 267:(1) 89-105.
- Ong KJ, MacCormack TJ, Clark RJ, Ede JD, Ortega V a., Felix LC, Dang MKM, Ma G, Fenniri H, Veinot JGC, Goss GG. 2014. Widespread nanoparticle-assay interference: Implications for nanotoxicity testing. *PLoS One* 9:(3).
- Peng M, Li H, Luo Z, Kong J, Wan Y, Zheng L, Zhang Q, Niu H, Vermorken A, Van de Ven W, Chen C, Zhang X, Li F, Guo L, Cui Y. 2015. Dextran-coated superparamagnetic nanoparticles as potential cancer drug carriers in vivo. *Nanoscale* 7:(25) 11155-11162.
- Pérez-Hernández H, Pérez-Moreno A, Sarabia-Castillo CR, García-Mayagoitia S, Medina-Pérez G, López-Valdez F, Campos-Montiel RG, Jayanta-Kumar P, Fernández-Luqueño F. Ecological Drawbacks of Nanomaterials Produced on an Industrial Scale: Collateral Effect on Human and Environmental Health. *Water Air Soil Pollut*. 2021;232(10):435.
- Periasamy VS, Jegan A, Mohammad A, Khalid A, Ali A. 2014. Fe(3)O(4) nanoparticle redox system modulation via cell-cycle progression and gene expression in human mesenchymal stem cells. *Environ Toxicol* 24:(3) 296-303.
- Piccinno F, Gottschalk F, Seeger S, Nowack B. 2012. Industrial production quantities and uses of ten engineered nanomaterials in Europe and the world. *J Nanoparticle Res* 14:(9).
- Rahman MM, Lee JK, Jeong J, Seo YR. 2013. Usage of nanoparticles with their potential toxicity assessment and regulatory guidelines. *Toxicol. Environ. Health Sci* 5:(2) 49-54.

- Raninga P V, Trapani G Di, Tonissen KF. 2014. Cross talk between two antioxidant systems, Thioredoxin and DJ-1 consequences for cancer. *Oncoscience* 1:(1) 95-100.
- Ranjbary, A.G., Saleh, G.K., Azimi, M., Karimian F, Mehrzad J. and Zohdi J. 2023. Superparamagnetic Iron Oxide Nanoparticles Induce Apoptosis in HT-29 Cells by Stimulating Oxidative Stress and Damaging DNA. *Biol Trace Elem Res* 201, 1163–1173.
- Rutkowski DT, Kang S-W, Goodman AG, Garrison JL, Taunton J, Katze MG, Kaufman RJ, Hegde RS. 2007. The Role of p58IPK in Protecting the Stressed Endoplasmic Reticulum. *Mol Biol Cell* 18:(1) 3681-3691.
- Sharma G, Kodali V, Gaffrey M, Wang W, Minard KR, Karin NJ, Teeguarden JG, Thrall BD. 2014. Iron oxide nanoparticle agglomeration influences dose rates and modulates oxidative stress-mediated dose-response profiles in vitro. *Nanotoxicology* 8:(6) 663-75.
- Sikalidis AK, Mazor KM, Lee JI, Roman HB, Hirschberger LL, Stipanuk MH. 2014. Upregulation of capacity for glutathione synthesis in response to amino acid deprivation: regulation of glutamate-cysteine ligase subunits. *Amino Acids* 1-12.
- Silva AH, Lima E Jr, Mansilla MV, Zysler RD, Troiani H, Piscioti MLM, Locatelli C, Benech JC, Oddone N, Zoldan VC, Winter E, Pasa AA, Creczynski-Pasa TB. 2016. Superparamagnetic iron-oxide nanoparticles mPEG350- and mPEG2000-coated: cell uptake and biocompatibility evaluation. *Nanomedicine* 12(4):909-919.
- Singh N, Jenkins GJS, Asadi R, Doak SH. 2010. Potential toxicity of superparamagnetic iron oxide nanoparticles (SPION). *Nano Rev* 1:(0) 1-15.
- Soenen SJ, Cuyper M De. 2010. Assessing iron oxide nanoparticle toxicity in vitro: current status and future prospects. *Nanomedicine (Lond)* 5:(8) 1261-75.
- Sun B, Liu R, Ye N, Xiao Z-D. 2015. Comprehensive Evaluation of microRNA Expression Profiling Reveals the Neural Signaling Specific Cytotoxicity of Superparamagnetic Iron Oxide Nanoparticles (SPIONs) through N-Methyl-D-Aspartate Receptor. *PLoS One* 10:(3) e0121671.
- Tan Gana NH, Victoriano AFB, Okamoto T. 2012. Evaluation of online miRNA resources for biomedical applications. *Genes to Cells* 17:(1) 11-27.
- Tomankova T, Petrek M, Kriegova E. 2010. Involvement of microRNAs in physiological and pathological processes in the lung. *Respir Res* 11:(1) 159.
- Tsai JH, Chen HW, Chen YW, Liu JY, Lii CK. 2010. The protection of hepatocyte cells from the effects of oxidative stress by treatment with vitamin e in conjunction with DTT. *J Biomed Biotechnol* Article ID 486267.
- Vakili-Ghartavol R, Momtazi-Borojeni AA, Vakili-Ghartavol Z, Aiyelabegan HT, Jaafari MR, Rezayat SM, Arbabi Bidgoli S. Toxicity assessment of superparamagnetic iron oxide nanoparticles in different tissues. *Artif Cells Nanomed Biotechnol.* 2020 Dec;48(1):443-451.
- Wahajuddin, Arora S. 2012. Superparamagnetic iron oxide nanoparticles: Magnetic nanoplatforms as drug carriers. *Int J Nanomedicine*, 7:3445-3471.
- Wang Z. 2010. MicroRNA: A matter of life or death. *World J. Biol Chem* 1:(4) 41-54.
- Wei H, Hu Y, Wang J, Gao X, Qian X, Tang M. Superparamagnetic Iron Oxide Nanoparticles: Cytotoxicity, Metabolism, and Cellular Behavior in Biomedicine Applications. *Int J Nanomedicine.* 2021 Aug 31;16:6097-6113.
- Weldy CS, Luttrell IP, White CC, Morgan-stevenson V, Theo K, Beyer RP, Afsharinejad Z, Kim F, Chitaley K, Kavanagh TJ. 2012. Glutathione (GSH) and the GSH synthesis gene Gclm modulate vascular reactivity in mice. *Free Radic Biol Med* 53:(6) 1264-1278.
- Wells M a., Abid A, Kennedy IM, Barakat AI. 2011. Serum proteins prevent aggregation of Fe<sub>2</sub>O<sub>3</sub> and ZnO nanoparticles. *Nanotoxicology* 6:837-846.
- Xu J-K, Zhang F-F, Sun J-J, Sheng J, Wang F, Sun M. 2014. Bio and Nanomaterials Based on Fe<sub>3</sub>O<sub>4</sub>. *Molecules* 19:(12) 21506-21528.
- Yang L, Kuang H, Zhang W, Aguilar ZP, Xiong Y, Lai W, Xu H, Wei H. 2015. Size dependent biodistribution and toxicokinetics of iron oxide magnetic nanoparticles in mice. *Nanoscale* 7:(2) 625-636.

Yokoi T, Nakajima M. 2011. Toxicological implications of modulation of gene expression by microRNAs. *Toxicol Sci* 123:(1) 1-14.

Zhang H, Liu H, Davies KJA, Sioutas C, E. CF, Morgan TE, Forman HJ. 2012. Nrf2-regulated phase II enzymes are induced by chronic ambient nanoparticle exposure in young mice with age-related impairments. *Free Radic Biol Med* 52:(2) 257-65.

Zhu M-T, Wang B, Wang Y, Yuan L, Wang H-J, Wang M, Ouyang H, Chai Z-F, Feng W-Y, Zhao Y-L. 2011. Endothelial dysfunction and inflammation induced by iron oxide nanoparticle exposure: Risk factors for early atherosclerosis. *Toxicol Lett* 203:(2) 162-171.

	SPION ( $\mu\text{g/mL}$ )	Hydrodynamic diameter (nm)	Zeta potential (mV)
Water	21	72.3 $\pm$ 1.9	-22.8 $\pm$ 0.9
	31	72.2 $\pm$ 1.5	-24.2 $\pm$ 1.4
	46	74.9 $\pm$ 5	-25.6 $\pm$ 1.9
	68	81.4 $\pm$ 14.9	-24.0 $\pm$ 1.2
	100	71.7 $\pm$ 0.9	-31.2 $\pm$ 0.9
	Mean	74.5 $\pm$ 1.8	-25.6 $\pm$ 1.5
DMEM 5% FBS	21	98.3 $\pm$ 5.9	-11.3 $\pm$ 0.2
	31	94.3 $\pm$ 6.5	-10.7 $\pm$ 0.4
	46	81.8 $\pm$ 1.1	-10.9 $\pm$ 0.4
	68	85.9 $\pm$ 0.6	-10.4 $\pm$ 0.2
	100	100.1 $\pm$ 1.1	-11.6 $\pm$ 0.3
	Mean	92.1 $\pm$ 3.5	-11.0 $\pm$ 0.2

Table 1: Hydrodynamic particle size distributions measured by DLS and zeta potential values. Solutions obtained under various conditions in both water and DMEM with 5% FBS.

ID	Gene Symbol	Gene Name	Fold-change (95% CI)	p value*
601176	<i>GCLM</i>	glutamate-cysteine ligase, modifier subunit	1.6 (1.24 - 2.00)	0.011
601112	<i>TXNRD1</i>	thioredoxin reductase 1	1.5 (1.35 - 1.73)	0.001
601184	<i>DNAJC3</i>	dnaJ (Hsp40) homolog, subfamily C, member 3	1.5 (1.14 - 1.88)	0.022
601530	<i>SQSTM1</i>	sequestosome 1	1.4 (1.11 - 1.72)	0.041
108355	<i>GRB2</i>	growth factor receptor-bound protein 2	1.3 (1.11 - 1.57)	0.037
611595	<i>TXNL4B</i>	thioredoxin-like 4B	1.3 (1.16 - 1.44)	0.009
603612	<i>TNFRSF10B</i>	tumor necrosis factor receptor superfamily, member 10b	1.2 (1.11 - 1.29)	0.008
134660	<i>GSTP1</i>	glutathione S-transferase pi 1	1.1 (1.06 - 1.21)	0.017

Table 2: Significant gene expression changes in HepG2 cells after 72h SPION exposure

\*Student's t-test; p<0.05 considered as significant.

ID	miRNA	Fold-change (95% CI)	p value*
300568	mir-221	0.8 (1.44 - 1.41)	0.343
611020	mir-21	1.1 (1.32 - 0.85)	0.621
612092	mir-200c	1.1 (0.94 - 0.77)	0.722
609416	mir-17-5p	0.9 (1.35 - 0.85)	0.240
600566	mir-146a	1.1 (1.19 - 1.09)	0.754
605386	let-7a	1.4 (0.97 - 0.73)	0.244

Table 3: miRNA expression changes in HepG2 cells exposed to SPION after 72h incubation

\*Student's t-test; p<0.05 considered as significant

## FIGURES CAPTIONS

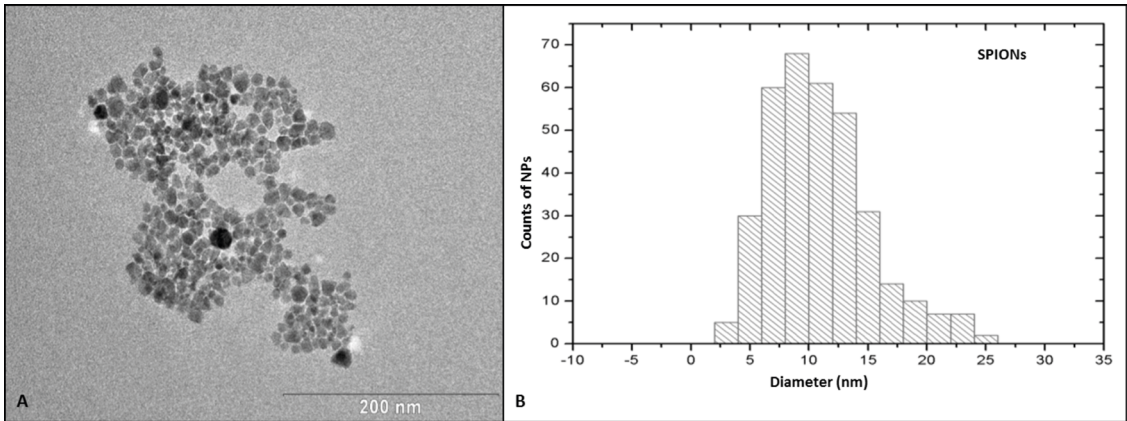


**Figure 1:** Morphological and size characterization of SPION. (A) Representative TEM image of spherical SPION in water. (B) Distribution of SPION diameters measured by TEM images with mean size of  $10.9 \pm 4.32$  nm.

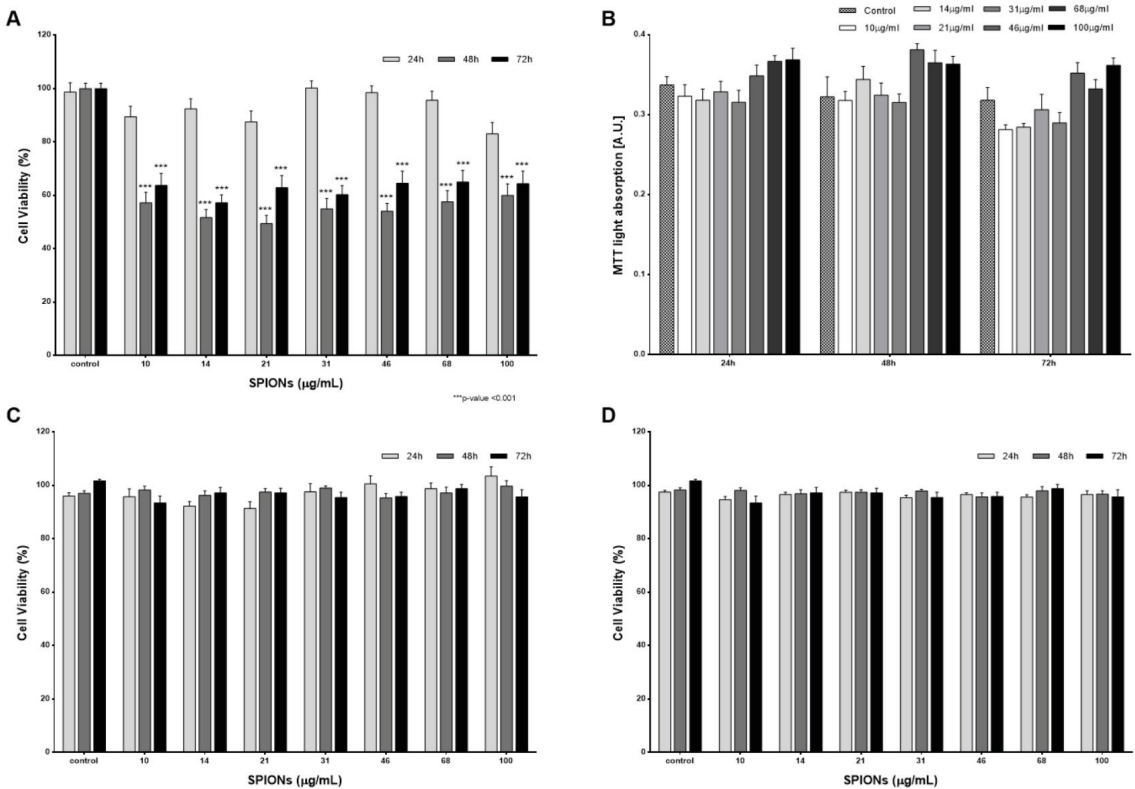


**Figure 2:** Cell viability evaluated by MTT assay for HepG2 cells after 24, 48 and 72h exposure with increasing concentrations of SPION (10, 14, 21, 31, 46, 68 and 100 µg/mL). Statistical significance was determined by one-way ANOVA test with  $p < 0.001$  considered as highly significant (\*\*\*) .

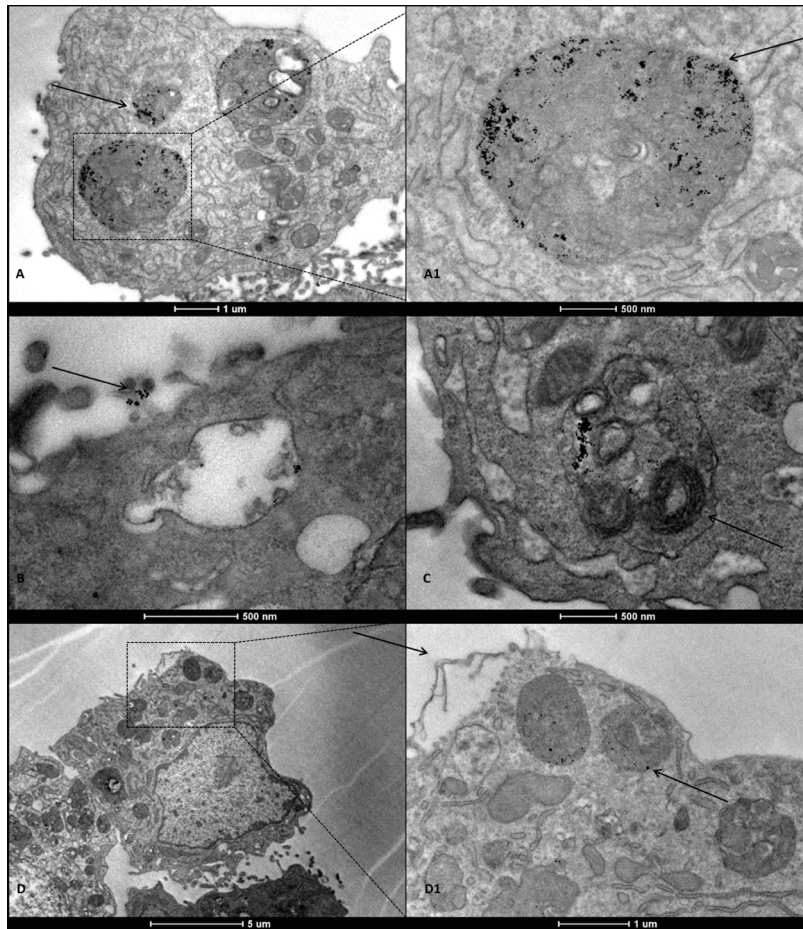


**Figure 3:** Transmission electron microscopy (TEM) images of HepG2 cells after 72h exposure to SPION.

(A) Uptake of SPION by cells exposed to 100 $\mu$ g/ml of NPs. (A1) Inset shows SPION in a vesicle at higher magnification. (B) NPs distributed on cell membrane surface after 100 $\mu$ g/ml of SPION exposure. (C) Myelin figures in the cytoplasm of cells exposed to 46 $\mu$ g/ml of SPION. (D) Plasma membrane blebbing formation in cells exposed to 68 $\mu$ g/ml of SPION. (D1) Inset shows a higher magnification of membrane blebbing and SPION in vesicles.

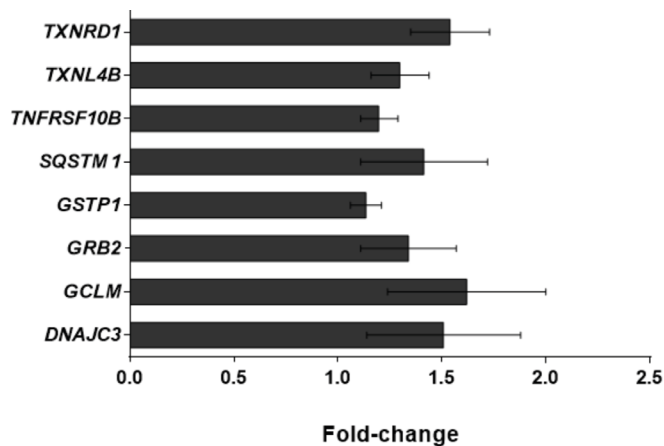


**Figure 4:** mRNA analysis of HepG2 cells after 72h incubation with 10 $\mu$ g/mL of SPION. Significant gene expression changes were verified comparing to control group.  $p < 0.05$  considered as significant.

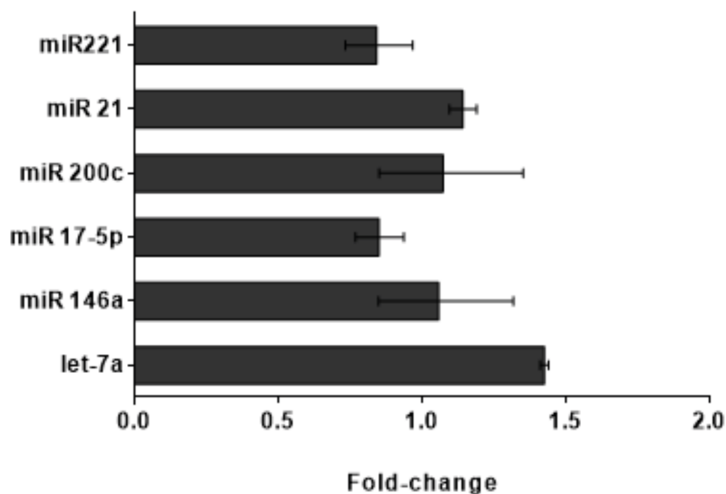


**Figure 5:** miRNA analysis of HepG2 cells exposed to 10µg/mL of SPION after 72h incubation. Data are expressed as fold change.

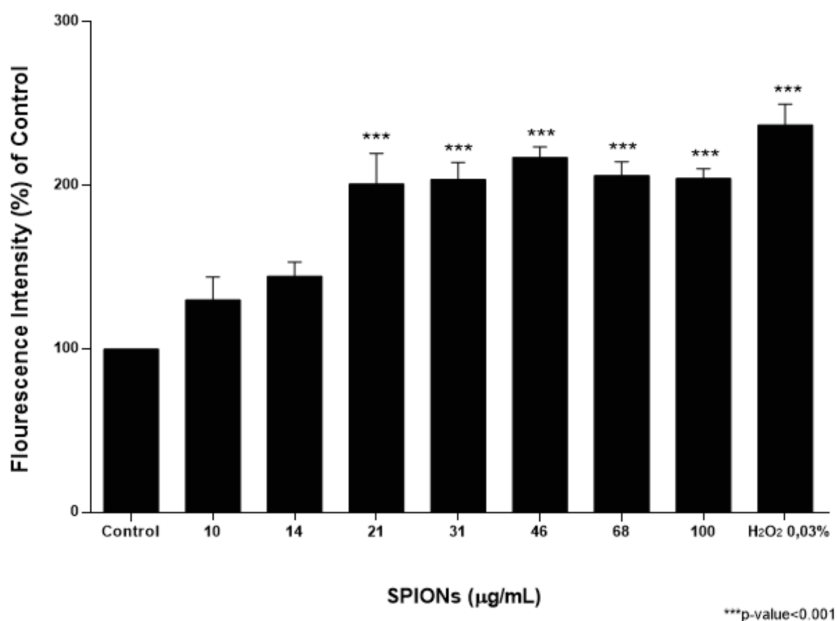


**Figure 6:** Intracellular ROS levels measurement. The exposure to 21, 31, 46 and 100µg/ml of SPION after 72h significantly induced increase in intracellular ROS levels in HepG2 cells. Data are reported as percentage in flourescence intensity relative to control cells cultured in SPION-free media. p<0.05 considered as significant.

